Complex fabric development revealed by englacial seismic reflectivity: Jakobshavn Isbræ, Greenland

H. J. Horgan,[1] S. Anandakrishnan,[1] R. B. Alley,[1] L. E. Peters,[1] G. P. Tsoflias,[2] D. E. Voigt,[1] and J. P. Winberry[1]

Received 19 February 2008; revised 23 March 2008; accepted 17 April 2008; published 21 May 2008.

[1] High-resolution reflection seismic data from Jakobshavn Isbræ, Greenland, reveal complex fabric development. Abundant englacial reflectivity occurs for approximately half the thickness of the ice (the lower half), and disruption of the englacial reflectors occurs in the lower 10–15% of the ice-thickness. These depths correspond to the higher impurity-content, and more easily deformed, ice from the Younger Dryas and Last Glacial Maximum to Stage-3. We conclude that the reflectivity results from contrasting seismic velocities due to changes in the crystal orientation fabric of the ice, and suggest that these fabric changes are caused by variations in impurity loading and subsequent deformation history. These findings emphasize the difference between ice-divide and ice-stream crystal orientation fabrics and have implications for predictive ice sheet modeling. **Citation:** Horgan, H. J., S. Anandakrishnan, R. B. Alley, L. E. Peters, G. P. Tsoflias, D. E. Voigt, and J. P. Winberry (2008), Complex fabric development revealed by englacial seismic reflectivity: Jakobshavn Isbræ, Greenland, *Geophys. Res. Lett.*, *35*, L10501, doi:10.1029/2008GL033712.

1. Introduction and Data

[2] Jakobshavn Isbræ highlights the uncertainty surrounding the role of ice dynamics in ice-sheet decay and sea level rise – Greenland is thinning around the margins, and Jakobshavn has recently experienced large accelerations in flow speed [*Alley et al.*, 2005; *Thomas et al.*, 2003; *Joughin et al.*, 2004]. Jakobshavn is Greenland's fastest glacier, with speeds of up to 12,600 m a^{-1} observed in 2003 [*Joughin et al.*, 2004], and it drains approximately 6.5% of the Greenland Ice Sheet [*Echelmeyer et al.*, 1991]. In our study area (Figure 1), the ice is flowing towards the deep main trough of Jakobshavn Isbræ at ~200 m a^{-1}, and driving stress averages ~200 kPa.

[3] Internal deformation dominates Jakobshavn Isbræ's motion within the deep central trough and contributes significantly outside the trough [*Echelmeyer et al.*, 1991; *Iken et al.*, 1993; *Funk et al.*, 1994; *Lüthi et al.*, 2002], although basal sliding and subglacial deformation doubtlessly contribute. Here we present active-source seismic data that image the internal structure at a location ~85 km upstream of the grounding line of Jakobshavn Isbræ, providing an unprecedented view of fabric development within this glacier.

1.1. Data Acquisition

[4] Multichannel-seismic-data were acquired in May 2007 along two orthogonal profiles, 10 km and 6 km long, oriented parallel and perpendicular to the flow of the glacier, respectively (Figure 1). The seismic sources were provided by the detonation of 500 g of PETN (pentaerythritol tetranitrate) at a depth of 10 m below the surface. Twenty-four vertical-component geophones were placed at a spacing of 20 m along the profiles. The minimum and maximum shot–receiver offsets were 10 m and 470 m, respectively. We used 28-Hz single-component geophones for recording all data, except for the downstream 2 km of the longitudinal profile, where 40 Hz "georods" were used instead. (A georod is an instrument developed specifically for recording in snow and firn, and consists of 4 geophone elements spaced vertically 20 cm apart in a high-density plastic housing.) The shot spacing was 160 m for the longitudinal profile and 240 m for the transverse profile (resulting in a nominal fold of 1.5 and 1 respectively). Data were recorded on a Geometrics Geode system with simultaneous shot triggering and data recording enabled by GPS synchronization. The dominant frequencies in our data of 50–200 Hz result in a quarter-wavelength vertical resolution of ~5–20 m.

1.2. Data Processing

[5] The data were edited to remove noisy and bad traces. Frequency filtering was applied with a band–pass of 20 to 300 Hz. Despiking was applied to remove noise due to crevassing events, which were apparent in the data as steeply-dipping linear arrivals. The shot data were then amplitude-balanced, normal-moveout corrected at a velocity of 3830 m s^{-1}, and sorted to common-depth-point gathers prior to stacking. No deconvolution was applied to the data because of the impulsive source and reflection signatures. Automatic-gain control was applied prior to plotting and in some cases the bed reflection was muted (e.g., Figure 2, inset) in order to better display the relatively lower amplitude englacial reflectors.

1.3. Profile Descriptions

[6] The longitudinal profile (Figure 2) shows englacial reflectivity in the lower half of the ice. Reflections may be present above this depth but if so they are masked by the source-generated noise. The englacial reflections are smooth and bed-conformable at long wavelengths, and are continuous along our profiles (the disruption at km 4.5 is due to low signal-to-noise ratio). Nearer the bed, one reflection has a markedly different character to the overlying internal

[1]Department of Geosciences, Pennsylvania State University, University Park, Pennsylvania, USA.
[2]Department of Geology, University of Kansas, Lawrence, Kansas, USA.

0094-8276/08/2008GL033712

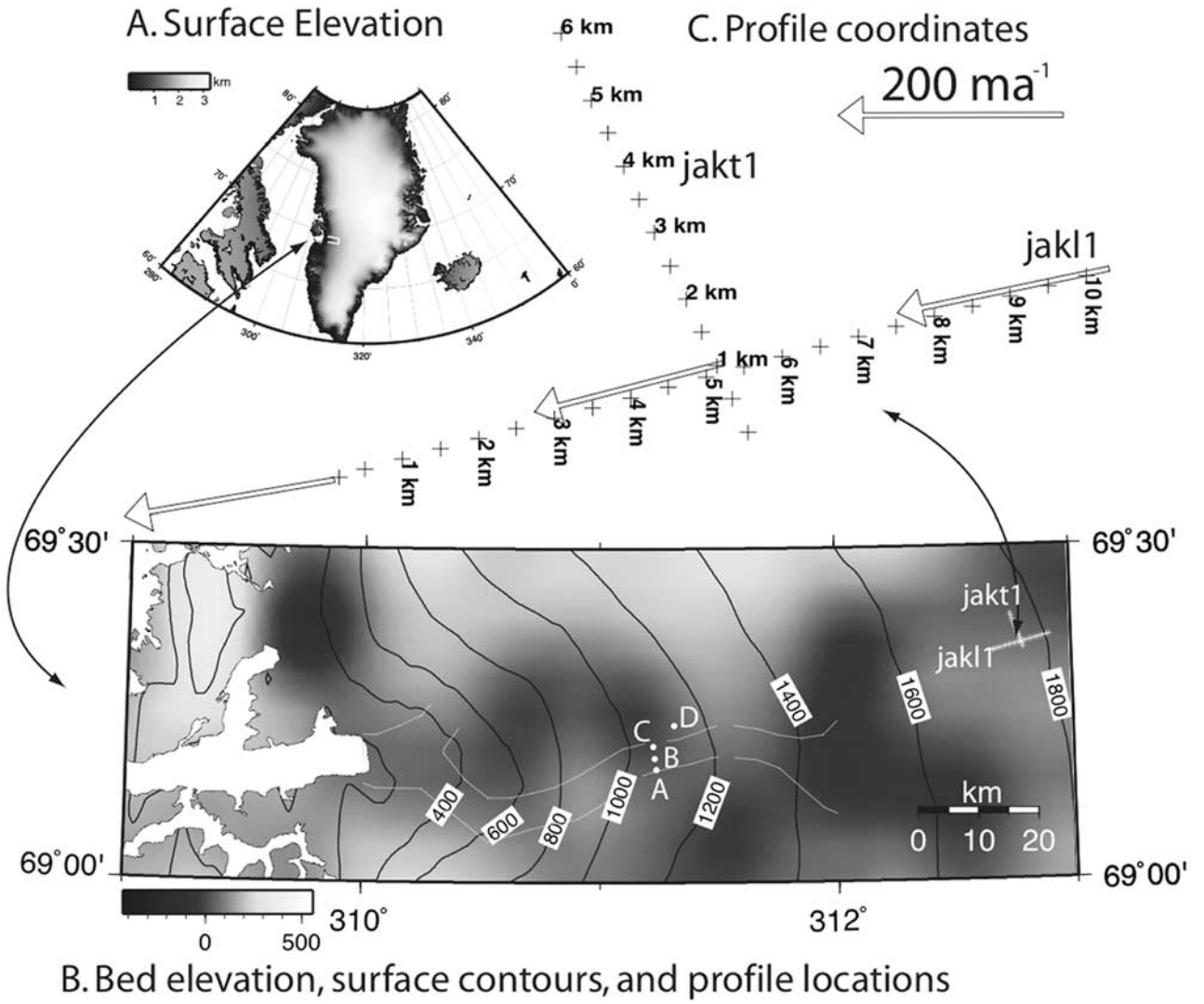

Figure 1. Study area location. (a) Greenland ERS-1 elevation data [*Bamber et al.*, 2001]; the box shows the location of Figure 1b. (a) Jakobshavn Isbræ with bed elevation (greyscale) and surface elevation (contours) [*Bamber et al.*, 2001]. White dots and letters show the locations of the drillsites of *Iken et al.* [1993] and *Lüthi et al.* [2002]. Also shown are the locations of the seismic lines reported here (white crosses) and the outline of the main trough of Jakobshavn. The trough is as shown by *Iken et al.* [1993], *Funk et al.* [1994], and *Lüthi et al.* [2002, 2003], and was delineated using seismic methods [*Clarke and Echelmeyer*, 1996], and is not evident in the work by *Bamber et al.* [2001]. (c) Seismic profiles, distance marks, and GPS-derived velocity vectors obtained from occupations during our field campaign.

reflectors: it is of low frequency and high amplitude. This low-frequency arrival is at an average height above the bed of 270 ± 40 m or ∼15% of the ice thickness of 1830 ± 110 m. (All thicknesses were calculated using a constant ice velocity of 3830 m s^{-1} determined from the relationship of *Kohnen* [1974] and assuming an average temperature of −15°C. Uncertainties represent the one standard-deviation distribution of the thickness along the profile.) Below the low-frequency reflector there is a relatively transparent layer (which is not due to auto-gain-control shadowing) followed by a series of discontinuous and chaotic internal layers throughout the lowest 190 ± 30 m (∼10%) of the ice.

[7] The transverse profile (Figure 3) matches the englacial reflectivity of the longitudinal profile but the horizontal wavelengths of the layer undulations are shorter. The length-to-amplitude ratio for the longitudinal profile is ∼200:1, and for the transverse profile is ∼30:1. In the transverse profile, the reflectivity is generally bed-conformable. As in the longitudinal profile, both the deep low-frequency arrival and the disturbed layer near the bed are present. The low-frequency arrival averages 260 ± 30 m off the bed (14% of the ice thickness of 1850 ± 40 m) and the disturbed layer is the lower 170 ± 30 m (9% of the ice thickness).

2. Discussion

2.1. The Origin of Englacial Reflectivity

[8] Observations of englacial seismic reflectivity have been made in Antarctica, where they have been variously attributed to the entrainment of basal sediment [*Bentley*,

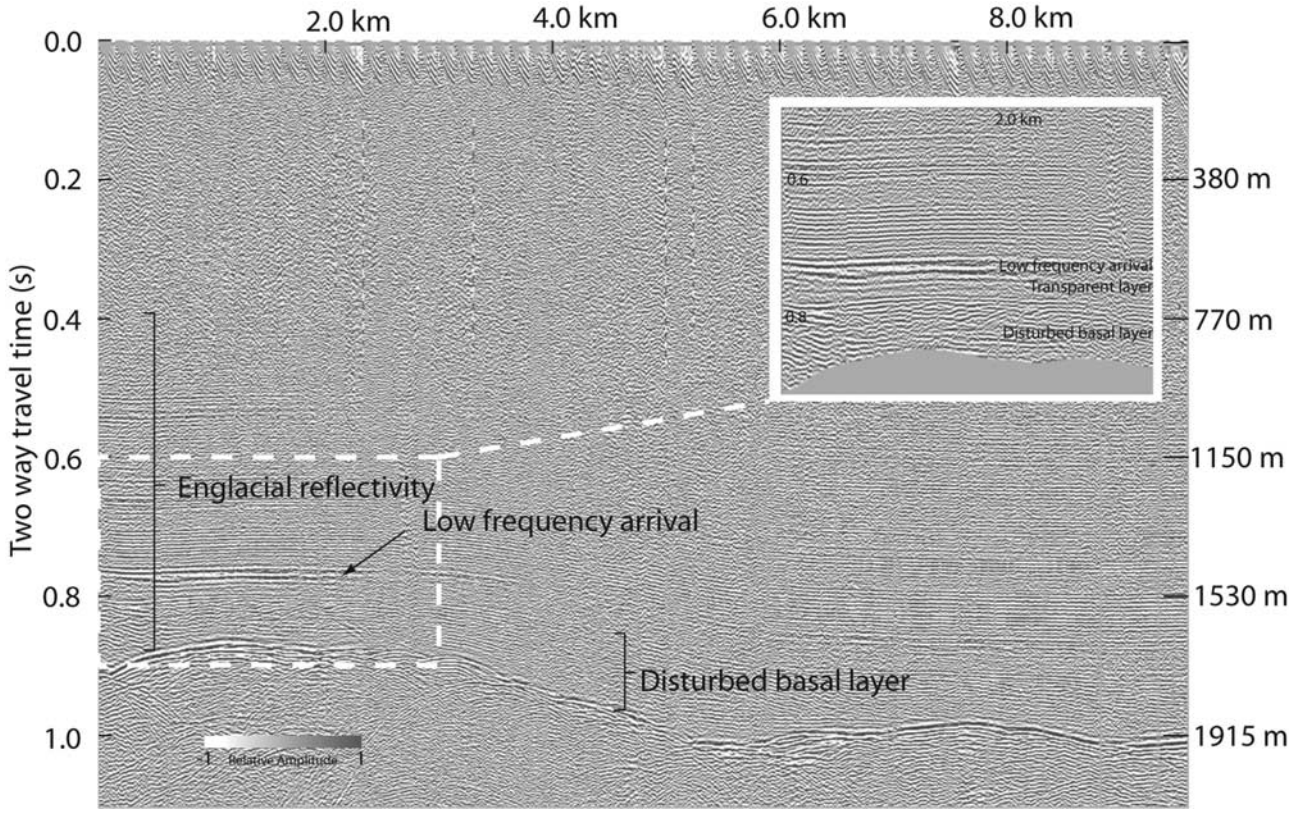

Figure 2. The longitudinal multichannel seismic profile jakl1. The left axis shows two-way travel-time, while the right axis shows depth converted at an ice velocity of 3830 m s^{-1}. The horizontal axis shows distance along the profile in km. Flow is from right to left, and the transverse profile crosses at ~5 km. Inset: zoom on the internal reflectivity near the bed of jakl1; an end mute has been applied to keep the high-amplitude bed arrival from masking the internal reflectors in the basal layer.

1971; *Smith*, 1996] or to changes in crystal orientation fabrics [*Blankenship and Bentley*, 1987; *Anandakrishnan*, 1996; *Burkett*, 2000].

[9] The seismic reflection coefficient is determined by contrasts in acoustic impedance (z), which is the product of density (ρ) and velocity (v) ($z = \rho v$). The density of ice is relatively constant at these depths (>900 m) [e.g., *Gow et al.*, 1997] and entrained rock is unlikely: debris is only observed in the very lowest 10's of meters at the ice divide [*Gow et al.*, 1997] and there is no transport mechanism known to be capable of entraining material higher up in the ice column. Furthermore, debris is not observed far above the bed in icebergs or boreholes. The seismic velocity of ice can vary due to a number of reasons, which we detail below. Seismic velocity (V_p) is weakly dependent on temperature (T) ($V_p = -(2.30 \pm 0.17)\mathrm{T} + 3795$ m s^{-1} [*Kohnen*, 1974]). However, even the high temperature-gradients observed in boreholes near our study area [*Iken et al.*, 1993; *Lüthi et al.*, 2002] are insufficient to produce discernible velocity contrasts. Velocity is, however, highly anisotropic in single-crystal ice, with 5% differences observed between the slow *a* and the fast *c*-axis [*Röthlisberger*, 1972]. Glacier ice can range from isotropic to nearly single-crystal anisotropy [e.g., *Blankenship and Bentley*, 1987; *Anandakrishnan et al.*, 1994]. We propose that contrasting degrees of anisotropy, brought about by variations in crystal orientation fabric, are responsible for the observed reflectivity.

2.2. Crystal Orientation Fabric

[10] Typically, near the surface in the center of an ice sheet, the *c*-axis distribution is random or weakly clustered about the vertical [e.g., *Diprinzio et al.*, 2005]. With increasing depth, *c*-axes are typically rotated to the vertical (by vertical compression or bed-parallel simple shear) or toward a vertical plane (by vertical compression with convergent flow [e.g., *Wang et al.*, 2002]). Near the base of an ice sheet, recrystallization can result in a return to a dispersed *c*-axis distribution within a cone angle of ~30–35° [*Alley*, 1988; *Budd and Jacka*, 1989]. Under strong basal shear, recrystallization may create multi-pole fabrics that are not symmetrical about the vertical [*Kamb*, 1972]. Recrystallization is favored by higher temperatures, higher strain rates, and lower impurity (dust) loading, which together create new strain-free nuclei, the driving stress for growth of those nuclei, and the ability for boundaries of those nuclei to migrate into strained ice [*Alley et al.*, 1995; *Budd and Jacka*, 1989]. In the event of contrasts in impurity loading, *c*-axis-vertical fabrics in fine-grained impure ice are found adjacent to recrystallized fabrics in coarser-grained, purer ice [e.g., *Gow and Meese*, 2007].

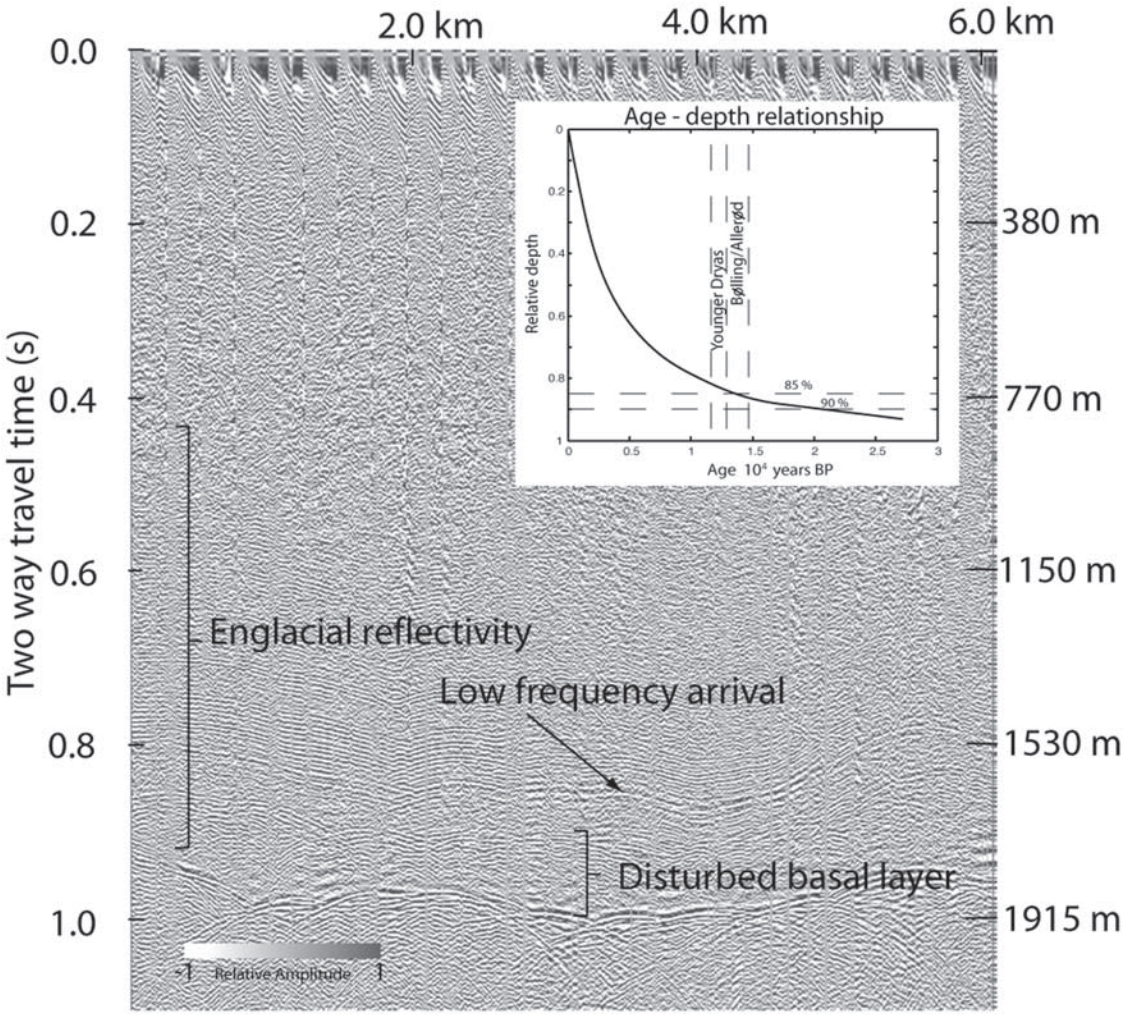

Figure 3. The transverse multichannel profile jakt1. The left axis shows two-way travel time, while the right axis shows depth converted at an ice velocity of 3830 m s^{-1}. The horizontal axis shows distance along the profile in km. Flow is into the page, and the longitudinal profile crosses at ~1 km. Inset: age–depth relationship (see text for discussion). Also shown in the inset are dashed lines at 85% and 90% of the ice thickness and time-lines representing the timing of the Younger Dryas and Bølling-Allerød (timing from *Alley et al.* [1993]).

[11] In order to fit the observations of internal reflectivity made here, we require the fabric to successively switch from one style to another down through the ice column. Such switching is not commonly observed in ice cores but is not unknown [e.g., *Gow et al.*, 1997; *Wang et al.*, 2002; *Diprinzio et al.*, 2005; *Gow and Meese*, 2007]. The viscosity of an ice crystal is dependent on the crystal orientation and small variations in fabric will be amplified with increasing strain as favorably oriented crystals deform more easily [e.g., *Alley*, 1988]. Variations in impurity loading, which at ice divides often do not manifest themselves as fabric variations, would respond differently to strain as they travel down-flow from the ice divide, eventually resulting in the fabric variations we interpret here.

2.3. Deforming Basal Layer and the Holocene–Wisconsin Transition

[12] An age–depth relationship (Figure 3 inset) was obtained from *Funk et al.* [1994] and verified by extending the internal layer tracing of *Legarsky and Gao* [2006] and *Gao* [2006]. Based on the age-depth relationship, on the considerations outlined above, and on knowledge of the impurity loading history of Greenland [*Mayewski et al.*, 1993; *O'Brien et al.*, 1995], we suggest that the low-frequency arrival corresponds to the bottom of the Younger Dryas stadial ice, with predominantly vertical *c*-axes, overlying purer Bølling-Allerød interstadial ice. The deeper zone of disrupted reflectors would then correspond to relatively impure Last Glacial Maximum (LGM) to Stage-3 ice, and might possibly record the effects of changes in impurity loading associated with Dansgaard-Oeschger events on the *c*-axis fabrics. The disruption in the basal layer is at least potentially similar to the deep disruption of layers in central Greenland cores related to ice flow processes [e.g., *Alley et al.*, 1997].

[13] Boreholes adjacent to and within the main trough of Jakobshavn have provided direct observations of the temperature structure and deformation [*Iken et al.*, 1993;

Funk et al., 1994; *Lüthi et al.*, 2002, 2003] (see Figure 1 for locations). In the ice sheet, *Lüthi et al.* [2002] observed enhanced deformation in a basal layer 150 m thick (~18% of the ice thickness), the top of which they correlated with the transition between Holocene and the relatively impure Wisconsin age ice. *Lüthi et al.* [2003] also hypothesize that thrust-faulting is occurring at the Holocene–Wisconsin interface. By matching borehole conductivity profiles, *Lüthi et al.* [2002] infer that a thicker layer of pre-Holocene ice exists within the main trough of Jakobshavn. This thicker layer should be resolvable using seismic reflection techniques.

[14] The internal reflectivity above the low-frequency arrival occurs in relatively pure Holocene ice, the reflections are low amplitude, and we suggest they result from one or a combination of the following: i) The impurity loading in Holocene ice is low but is not constant [*O'Brien et al.*, 1995], so dirtier ice may be holding the *c*-axis vertical while cleaner ice is recrystallizing; ii) Thin regions of high impurity loading related to volcanic events [*Zielinski et al.*, 1996] may be resulting in a correspondingly strong *c*-axis preference (similar to that observed by *Gow and Meese* [2007]) and corresponding reflection events; or iii) We may be imaging cyclic-behavior whereby *c*-axis orientations tend toward the vertical, strain accumulates, recrystallization occurs, and the cycle repeats. We know of no reports of similar internal reflectivity, which is almost certainly due to changes in *c*-axis fabric, from elsewhere on ice sheets, nor do we know of any prediction of the occurrence of such features. Understanding this new phenomenon may provide new insights into ice deformation and prove important for predictive ice sheet modeling.

3. Summary and Conclusions

[15] Complex fabric development is interpreted upstream on Jakobshavn Isbræ, Greenland, using active-source seismic methods. Englacial reflectivity is observed along two orthogonal profiles totaling 16 km in length. The englacial reflectivity has a long spatial-wavelength and is bed-conformable in the along-flow direction, while the reflectivity has a shorter spatial-wavelength perpendicular to flow. We argue that the reflectivity results from successive changes in crystal orientation fabric. In turn, these contrasting fabrics are thought to result from contrasts in impurity loading and subsequent differing responses to strain. A prominent reflector corresponds to impure Younger Dryas aged ice, and the discontinuous and chaotic reflectors near the base correspond to LGM to Stage-3 ice, where enhanced deformation is occurring. These results have particular importance for studies of fabric development and predictive ice sheet modelling.

[16] **Acknowledgments.** This work was made possible by the National Science Foundation and the Center for Remote Sensing of Ice Sheets (CReSIS) (NSF-OPP-0424589 (CReSIS), 0531211 (RBA), 0539578 (RBA)) along with field support from VECO Polar Resources and Air Greenland. We are grateful for careful reviewing by Andrew M. Smith and Martin Truffer, and for discussions with Martin Lüthi, Martin Funk, and the Penn State Ice Group. We are additionally grateful to Martin Funk for hosting HJH at Versuchsanstalt für Wasserbau, Hydrologie und Glaziologie (VAW), ETH, Zürich during a portion of HJH's work on this manuscript.

References

Alley, R., A. Gow, and D. Meese (1995), Mapping *c*-axis fabrics to study physical processes in ice, *J. Glaciol.*, *41*(137), 197–203.

Alley, R., A. Gow, D. Meese, J. Fitzpatrick, E. Waddington, and J. Bolzan (1997), Grain-scale processes, folding, and stratigraphic disturbance in the GISP2 ice core, *J. Geophys. Res.*, *102*(C12), 26,819–26,830.

Alley, R. B. (1988), Fabrics in polar ice sheets: Development and prediction, *Science*, *240*, 493–495.

Alley, R. B., P. U. Clark, P. Huybrechts, and I. Joughin (2005), Ice sheet and sea-level changes, *Science*, *310*, 456–460.

Alley, R. B., et al. (1993), Abrupt increase in Greenland snow accumulation at the end of the Younger Dryas event, *Nature*, *362*, 527–529.

Anandakrishnan, S. (1996), Seismic reflections from an internal layer: Fabric change or moraine?, *Eos Trans. AGU*, *77*, Spring Meet. Suppl., Abstract O12B-04.

Anandakrishnan, S., J. J. Fitzpatrick, R. B. Alley, A. J. Gow, and D. A. Meese (1994), Shear-wave detection of asymmetric *c*-axis fabrics in the GISP2 ice core, *J. Glaciol.*, *40*(136), 491–496.

Bamber, J., R. Layberry, and S. Gogineni (2001), A new ice thickness and bed data set for the Greenland ice sheet: 1. Measurement, data reduction, and errors, *J. Geophys. Res.*, *106*(D24), 33,773–33,780.

Bentley, C. (1971), Seismic evidence for moraine within the basal Antarctic ice sheet, in *Antarctic Snow and Ice Studies II, Antarct. Res. Ser.*, vol. 16, edited by A. P. Crary, pp. 89–129, AGU, Washington, D. C.

Blankenship, D. D., and C. R. Bentley (1987), The crystalline fabric of polar ice sheets inferred from seismic anisotropy, in *The Physical Basis of Ice Sheet Modeling*, edited by E. D. Waddington and J. S. Walder, *IAHS Publ.*, *170*, 17–28.

Budd, W. F., and T. H. Jacka (1989), A review of ice rheology for ice sheet modeling, *Cold Reg. Sci. Technol.*, *16*, 107–104.

Burkett, P. G. (2000), Ice fabric and active seismology: An investigation and interpretation in central West Antarctica, M. S. thesis, Pa. State Univ., Univ. Park.

Clarke, T. S., and K. A. Echelmeyer (1996), Seismic-reflection evidence for a deep subglacial trough beneath Jakobshavn Isbræ, West Greenland, *J. Glaciol.*, *42*(141), 219–232.

Diprinzio, C., L. Wilen, R. Alley, J. Fitzpatrick, M. Spencer, and A. Gow (2005), Fabric and texture at Siple Dome, Antarctica, *J. Glaciol.*, *51*(173), 281–290.

Echelmeyer, K. A., T. Clarke, and W. Harrison (1991), Surficial glaciology of Jakobshavn Isbræ, West Greenland: Part I. Surface morphology, *J. Glaciol.*, *37*(127), 368–382.

Funk, M., K. A. Echelmeyer, and A. Iken (1994), Mechanisms of fast flow in Jakobshavns Isbræ, West Greenland: Part II. Modeling of englacial temperatures, *J. Glaciol.*, *40*(136), 569–585.

Gao, X. (2006), Tracing of internal layers in radar echograms from a Greenland study region, M. S. thesis, Univ. of Mo., Columbia.

Gow, A., and D. Meese (2007), Physical properties, crystalline textures and *c*-axis fabrics of the Siple Dome (Antarctica) ice core, *J. Glaciol.*, *53*(183), 573–584.

Gow, A. J., D. A. Meese, R. B. Alley, J. J. Fitzpatrick, S. Anandakrishnan, G. A. Woods, and B. C. Elder (1997), Physical and structural properties of the GISP2 ice cores, *J. Geophys. Res.*, *102*(C12), 26,559–26,576.

Iken, A., K. Echelmeyer, W. Harrison, and M. Funk (1993), Mechanisms of fast flow in Jakobshavns Isbræ, West Greenland: Part I. Measurements of temperature and water level in deep boreholes, *J. Glaciol.*, *39*(131), 15–25.

Joughin, I., W. Abdalati, and M. Fahnestock (2004), Large fluctuations in speed on Greenland's Jakobshavn Isbræ glacier, *Nature*, *432*, 608–610.

Kamb, B. (1972), Experimental recrystallization of ice under stress, in *Flow and Fracture of Rocks, Geophys. Monogr. Ser.*, vol. 16, edited by H. Heard et al., pp. 211–241, AGU, Washington, D. C.

Kohnen, H. (1974), The temperature dependence of seismic waves in ice, *J. Glaciol.*, *13*(67), 144–147.

Legarsky, J., and X. Gao (2006), Internal layer tracing and age-depth relationship from the ice divide toward Jakobshavn, Greenland, *IEEE Geosci. Remote Sens. Lett.*, *3*(4), 471–475.

Lüthi, M., M. Funk, A. Iken, S. Gogineni, and M. Truffer (2002), Mechanisms of fast flow in Jakobshavns Isbræ, West Greenland: Part III. Measurements of ice deformation, temperature, and cross-borehole conductivity in boreholes to the bedrock, *J. Glaciol.*, *48*(162), 369–385.

Lüthi, M., M. Funk, and A. Iken (2003), Indication of active overthrust faulting along the Holocene-Wisconsin transition in the marginal zone of Jakobshavn Isbræ, *J. Geophys. Res.*, *108*(B11), 2543, doi:10.1029/2003JB002505.

Mayewski, P. A., L. D. Meeker, S. Whitlow, M. S. Twickler, M. C. Morrison, R. B. Alley, P. Bloomfield, and K. Taylor (1993), The atmosphere during the Younger Dryas, *Science*, *261*, 195–197.

O'Brien, S., P. Mayewski, L. Meeker, D. Meese, M. Twickler, and S. Whitlow (1995), Complexity of Holocene climate as reconstructed from a Greenland ice core, *Science*, *270*, 1962–1964.

Röthlisberger, H. (1972), Seismic exploration in cold regions, technical report, Cold Reg. Res. and Eng. Lab, Hanover, N. H.

Smith, A. M. (1996), Ice shelf basal melting at the grounding line, measured from seismic observations, *J. Geophys. Res.*, *101*(C10), 22,749–22,755.

Thomas, R., W. Abdalati, E. Frederick, W. Krabill, S. Manizade, and K. Steffen (2003), Investigation of surface melting and dynamic thinning on Jakobshavn Isbræ, Greenland, *J. Glaciol.*, *49*(165), 231–239.

Wang, Y., T. Thorsteinsson, J. Kipfstuhl, H. Miller, D. Dahl-Jensen, and H. Shoji (2002), A vertical girdle fabric in the NorthGRIP deep ice core, north Greenland, *Ann. Glaciol.*, *35*, 515–520.

Zielinski, G., P. Mayewski, L. Meeker, S. Whitlow, and M. Twickler (1996), A 110,000-Yr record of explosive volcanism from the GISP2 (Greenland) ice core, *Quat. Res.*, *45*(13), 109–118.

R. B. Alley, S. Anandakrishnan, H. J. Horgan, L. E. Peters, D. E. Voigt, and J. P. Winberry, Department of Geosciences, Pennsylvania State University, University Park, PA 16802, USA. (hhorgan@geosc.psu.edu)

G. P. Tsoflias, Department of Geology, University of Kansas, Lawrence, KS 66045, USA.